Cancer-Targeting Ultrasmall Silica Nanoparticles for Clinical Translation: Physicochemical Structure and Biological Property Correlations

*Feng Chen[1†], Kai Ma[2†], Miriam Benezra[1], Li Zhang[1], Sarah M. Cheal[1], Evan Phillips[1+], Barney Yoo[1], Mohan Pauliah[1], Michael Overholtzer[4,5], Pat Zanzonico[6], Sonia Sequeira[7], Mithat Gonen[8], Thomas Quinn[9], Ulrich Wiesner[2†, *], Michelle S. Bradbury[1,3†,*]*

[1]Department of Radiology, Sloan Kettering Institute for Cancer Research, New York, NY 10065, USA

[2]Department of Materials Science & Engineering, Cornell University, Ithaca, NY 14853, USA

[3]Molecular Pharmacology Program, Sloan Kettering Institute for Cancer Research, New York, NY 10065, USA

[4]Cell Biology Program, Sloan Kettering Institute for Cancer Research, New York, NY 10065, USA

[5]BCMB Allied Program, Weill Cornell Medical College, New York, NY 10065, USA

[6]Department of Medical Physics, Sloan Kettering Institute for Cancer Research, New York, NY 10065, USA

[7]Investigational Products Core, Sloan Kettering Institute for Cancer Research, New York, NY 10065, USA

[8]Department of Epidemiology and Biostatistics, Sloan Kettering Institute for Cancer Research, New York, NY 10065, USA

[9]Department of Biochemistry, University of Missouri, Columbia, MO 65211, USA

[†]FC and KM contributed equally to the work.

[*]MB and UW contributed equally to the work.

[+]Present address: Weldon School of Biomedical Engineering, Purdue University, West Lafayette, Indiana 47907 USA

Correspondence and requests for materials should be addressed to: M. S. Bradbury, email: bradburm@mskcc.org and U. Wiesner, email: ubw1@cornell.edu

Supplementary Figures and Tables

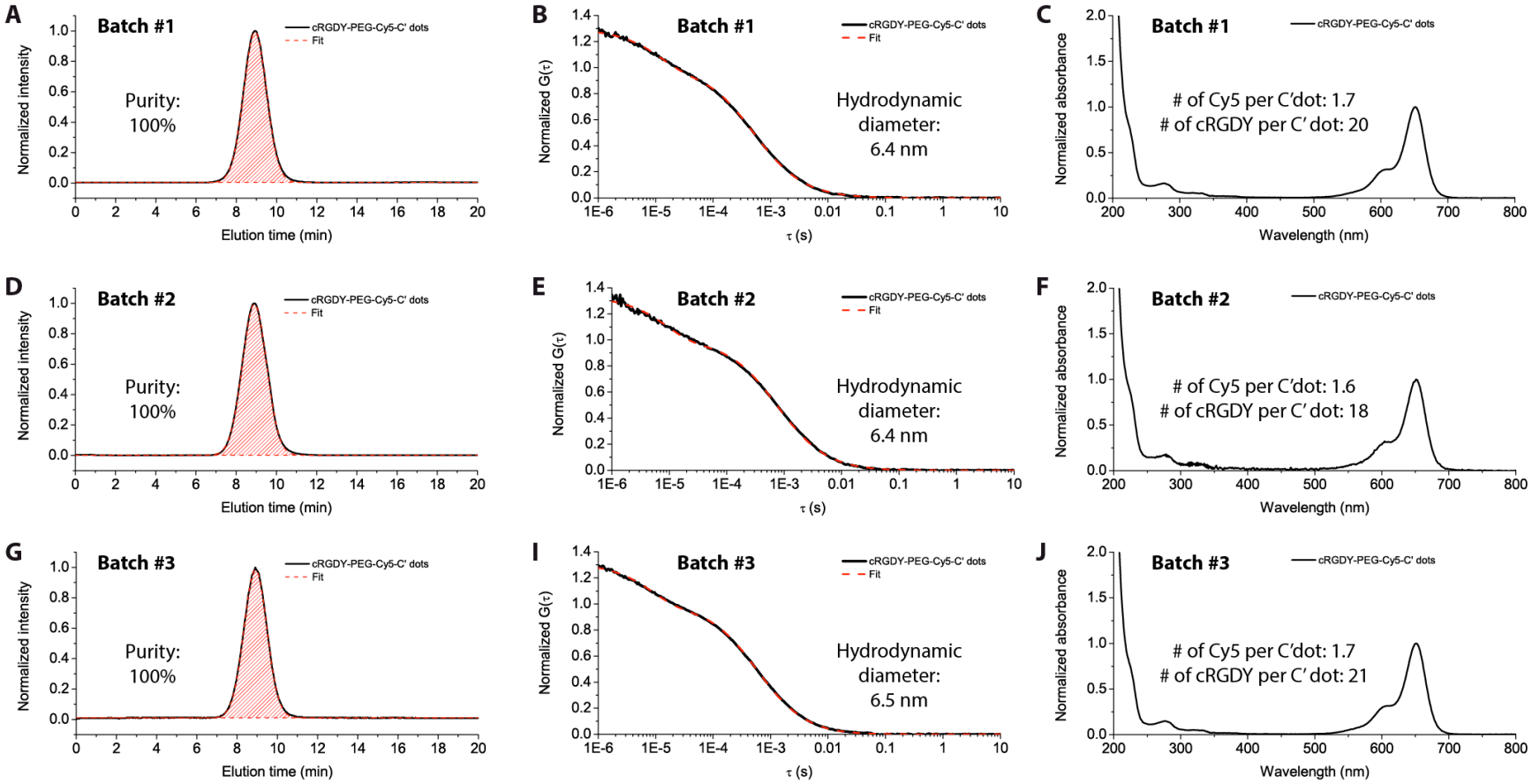

Figure S1. Batch-to-batch consistency of C' dot synthesis. GPC traces (A, D and G), FCS correlation curves (B, E and I), and UV-Vis absorbance spectra (C, F and J) of cRGDY-PEG-Cy5-C' dots from different batches, synthesized on different dates. Batch #2 (D to F) and #3 (G to J) were produced approximately 3 and 7 months after batch #1 (A to C), respectively.

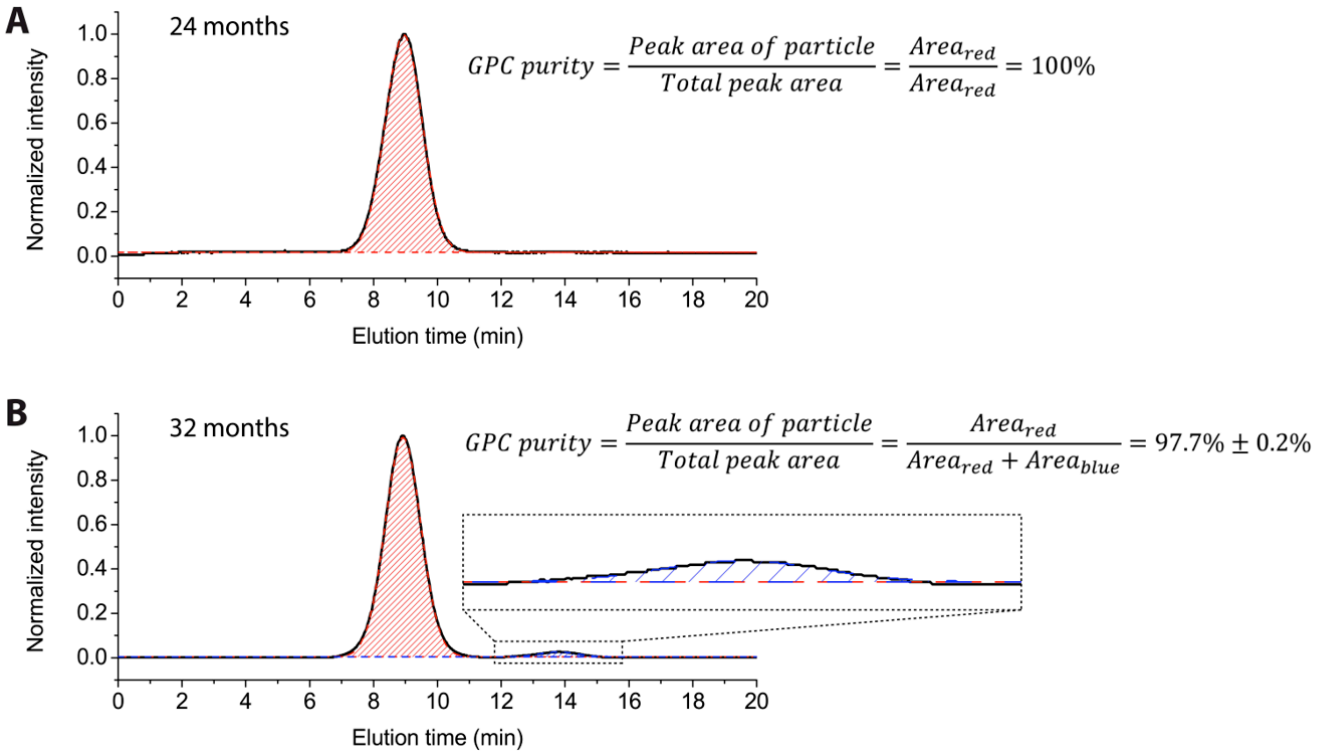

Figure S2. Comparison of GPC traces of cRGDY-PEG-Cy5-C' dots at different time points. GPC traces of cRGDY-PEG-Cy5-C' dots 24 months (A) and 32 (B) months after particle manufacture. The GPC peaks were fit using Gaussian distributions. The color code is the same as in Figure 1: Gaussian fit of main peak around 9 min is red, and second peak around 14 nm, attributed to an impurity with small molar mass, is blue. The GPC purity was assessed using the ratio of the peak area of the main particles to the total peak area in the GPC trace, as indicated in the figure. The GPC trace at 24 month (A) exhibited a single peak around 9 min, attributed to the C' dot particles. No impurity peak could be identified, indicating a 100% GPC purity (A). When there was only one peak in the GPC trace, no standard error was assigned to data from samples with 100% purity (see Figure 3H in main text). A second peak with elution time around 14 min started to appear after 24 months (fitted peak in B with blue color), likely due to the hydrolysis of PEG-silane on the C' dot surface, leading to the release of cRGDY peptide. Its intensity gradually increased to around 2% at 32 months after particle manufacture, resulting in a GPC purity of the C' dot product around 98% (B).

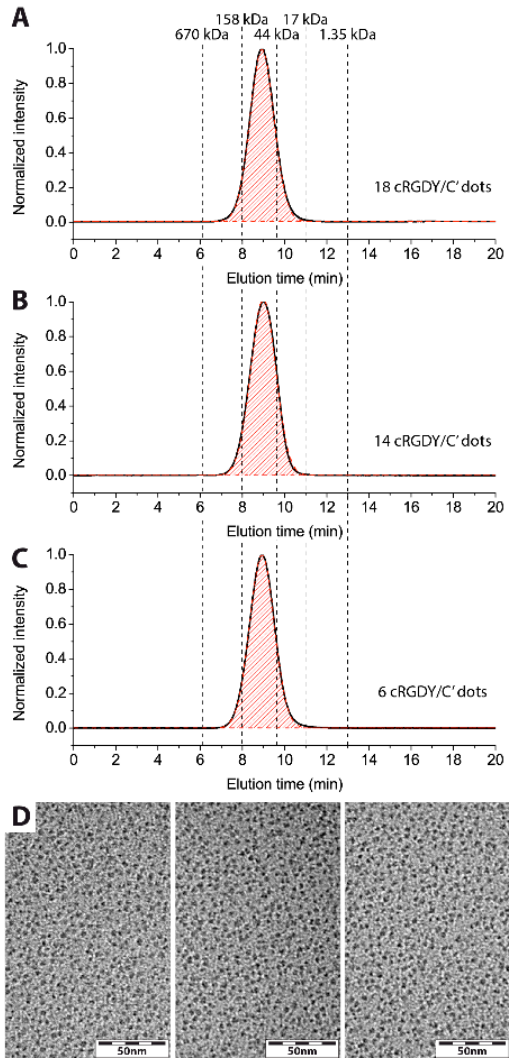

Figure S3. (A-C) GPC elugrams of cRGDY-PEG-Cy5-C' dot products with 18 (A), 14 (B) and 6 (C) cRGDY ligands per particle. (D) Representative TEM images of the C' dot products with 18 (left), 14 (middle) and 6 (right) cRGDY ligands per particle.

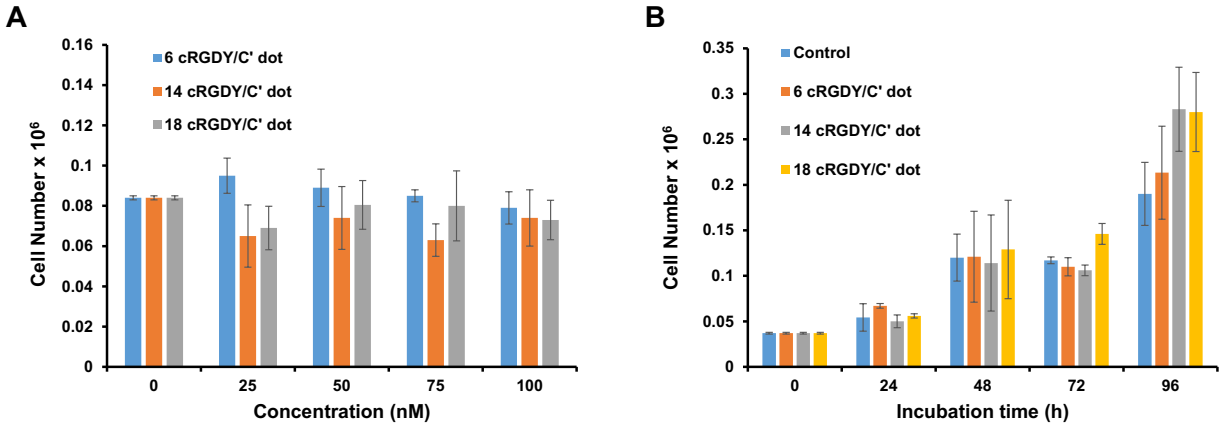

Figure S4. Viability and proliferation of M21 cells as a function of (A) particle concentration and (B) incubation time. A, B. Cell number as a measure of viability in subconfluent G0/G1-phase-synchronized M21 cells over a (A) 0 – 100 nM concentration range (48 hrs post-incubation) and (B) 96-hour time interval (~100 nM concentration) in media alone (zero point, 10% FBS) or after addition of particles bearing different ligand numbers in media supplemented with 10% FBS, as specified in A, B.

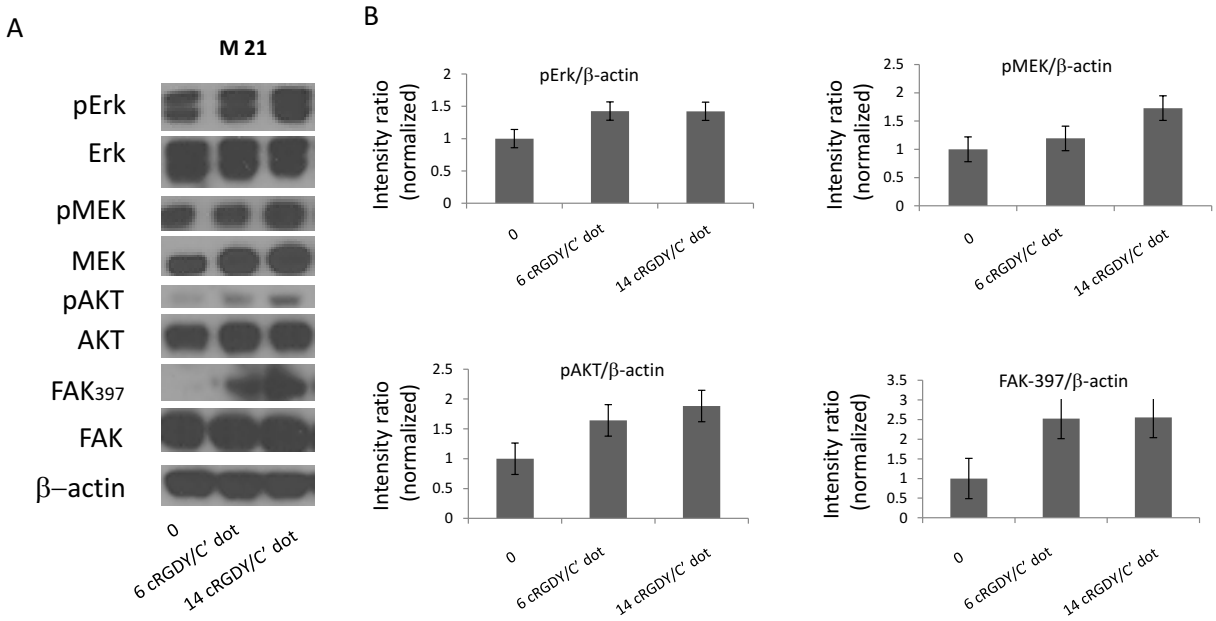

Figure S5. Cell signaling changes and corresponding fold differences as a function of ligand number in M21 cells. (A) Western blots of selected phosphorylated and total protein intermediates following M21 monolayer exposure to cRGDY-PEG-Cy5-C' dots (100 nM) bearing ~6 or 14 ligands in serum-deprived media (0.2% FBS), as against 0.2% FBS (control), over a 4-hr incubation time. β-actin blots served as controls. (B) Graphical summary of relative signal intensity changes of phospho-protein to β-actin (Adobe Photoshop; see Methods) for serum-deprived, particle-exposed cells versus serum-deprived cells.

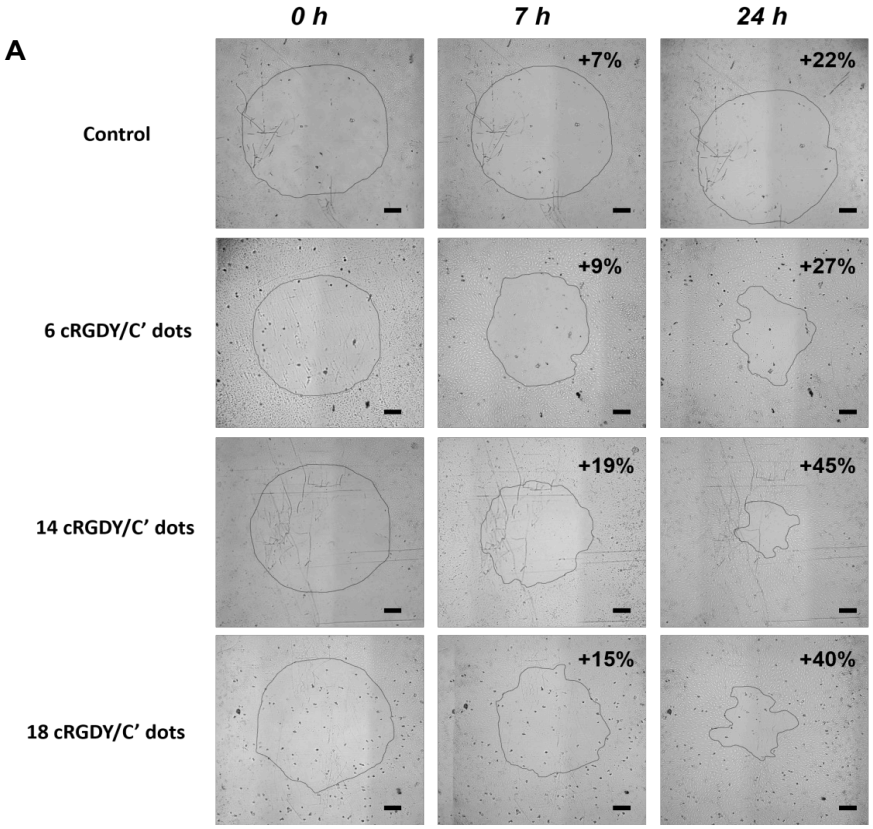

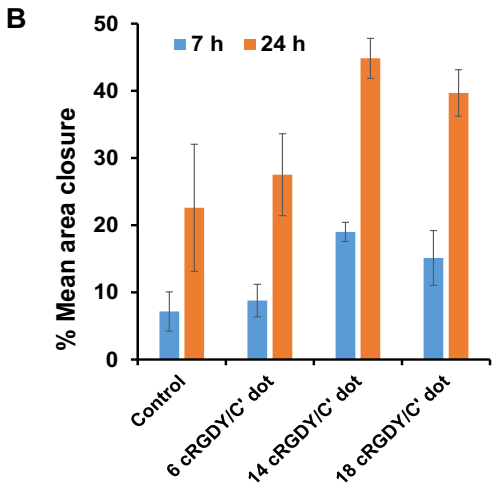

C

	P values	
	7 h	24 h
6 vs Control	0.229	0.225
14 vs Control	<0.001	<0.001
18 vs Control	0.003	0.002
14 vs 6	<0.001	<0.001
18 vs 6	0.011	0.001
18 vs 14	0.940	0.975

Figure S6. Effect of cRGDY-PEG-Cy5-C' dots on the cellular migration of HUVECs using time-lapse imaging. (A) Time-dependent changes in human umbilical vein endothelial cell (HUVEC) migration in ORIS™ collagen coated plates after exposing cells in EGM-2 medium with 0.2% FBS and growth factors-LONZA, to particles (400nM; 37°C) bearing a range of ligand numbers, as against 0.2% FBS supplemented media alone (control). Images were captured at time t=0 (pre-migration) and over a subsequent 24-hour time interval following stopper removal using a Zeiss Axiovert 200M inverted microscope (5x/.25NA objective) and a scan slide module (Metamorph® Microscopy Automation & Image Analysis Software). (B) Graphical plot of changes in the mean area of closure (%) as a function of particle ligand number for fixed concentrations using ImageJ software. Mean area of closure represents the difference in the area demarcated by the border of advancing cells (pixels) at arbitrary time points and after stopper removal (t=0), divided by the latter area. Triplicate assays were performed for each particle ligand number and time point. Scale bar in all images is 1 millimeter. (C) Tabulated p values based on two-sample t-tests.

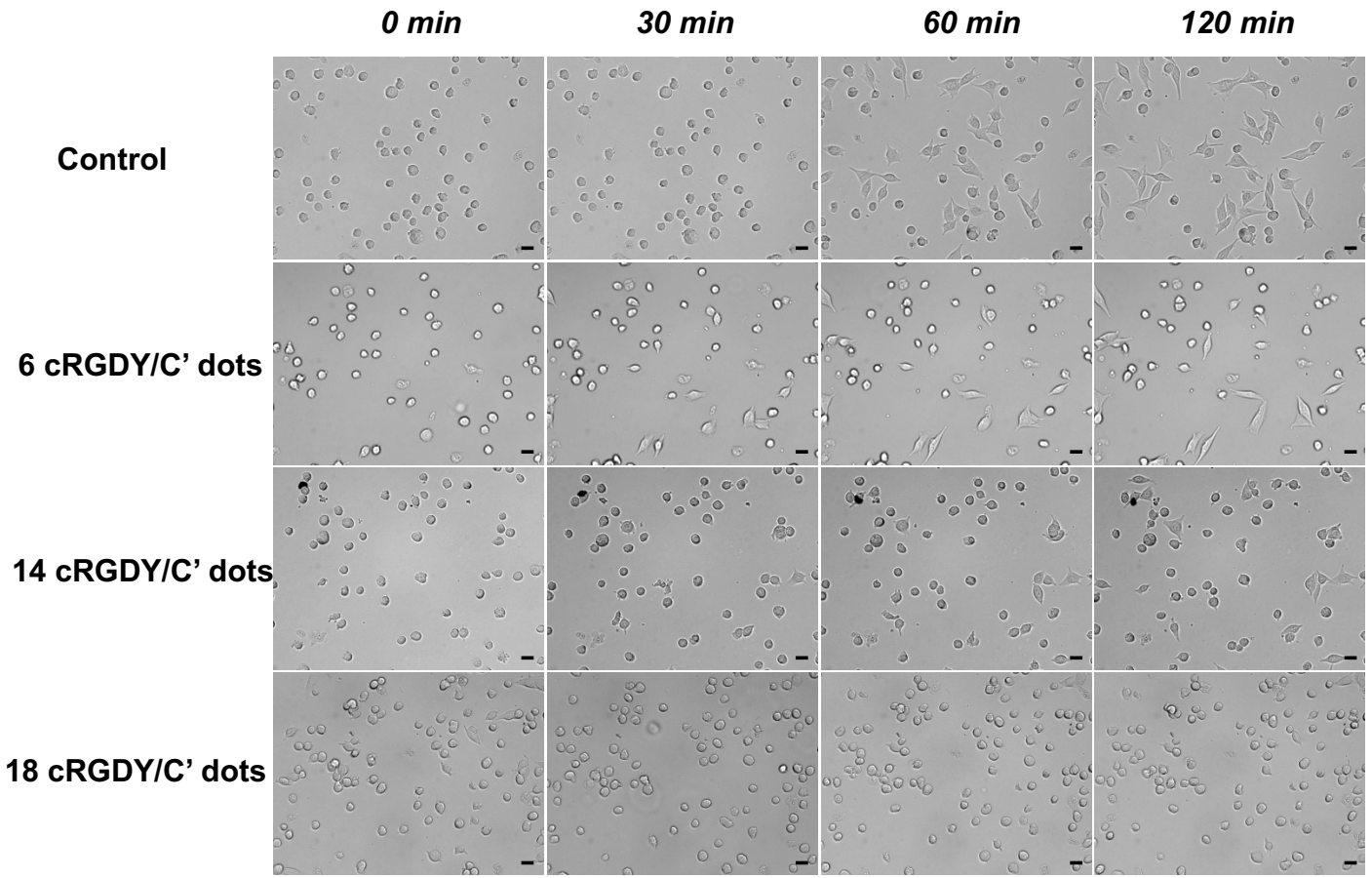

Figure S7. Modulation of M21 cell spreading and adhesion using cRGDY-PEG-Cy5-C' dots bearing different ligand numbers. (A) Time-lapse imaging showing changes in cellular attachment and spreading. Cells were pre-incubated in 0.2% FBS-supplemented RPMI (0.5 hour, 25 °C), without and with particles (400 nM), followed by seeding in (5 μg mL^{-1}) fibronectin-coated 96-well plates. Images were captured at t = 0, 0.5, 1, and 2 hrs using a Zeiss Axiovert 200M inverted microscope (20x /.4NA objective) and a scan slide module in Metamorph. Scale bar for all images is 30 μm.

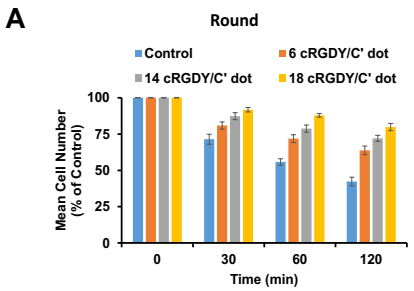

Time (min)	P values: Control vs 6	Control vs 14	Control vs 18	14 vs 6	18 vs 6	18 vs 14
30	<0.001	<0.001	<0.001	<0.001	<0.001	<0.001
60	<0.001	<0.001	<0.001	<0.001	<0.001	<0.001
120	<0.001	<0.001	<0.001	<0.001	<0.001	<0.001

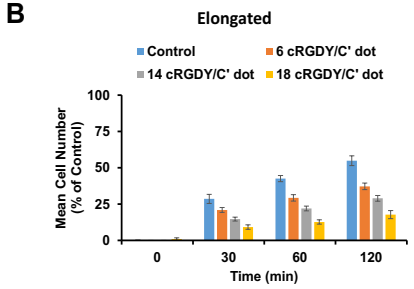

Time (min)	P values: Control vs 6	Control vs 14	Control vs 18	14 vs 6	18 vs 6	18 vs 14
30	<0.001	<0.001	<0.001	<0.001	<0.001	<0.001
60	<0.001	<0.001	<0.001	<0.001	<0.001	<0.001
120	<0.001	<0.001	<0.001	<0.001	<0.001	<0.001

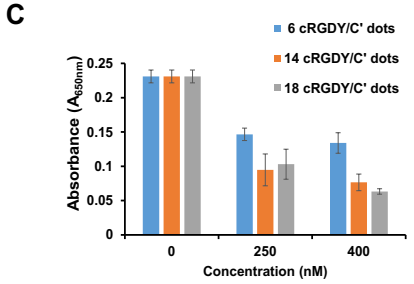

Concentration (nM)	P values: 14 v 6	18 v 6	18 v 14
250	<0.001	0.052	0.373
400	0.005	<0.001	0.185

Figure S8. Modulation of M21 cell spreading and adhesion using cRGDY-PEG-Cy5-C' dots bearing different ligand numbers. Graphical plots showing the mean number of (A, left) rounded and (B, left) elongated cells within 4 groups as a function of time: non-particle exposed and particle-exposed using 6 cRGDY/C' dot, 14 cRGDY/C' dot and 18 cRGDY/C' dot. Cells in each of three wells of a 96-well plate were manually counted in a minimum of three high power fields (200× magnification) and averaged. Tables in (A, right) and (B, right) show corresponding p values. (C, left) Absorbance (λ = 650 nm; SpectroMax M5 microplate reader) values for 4% paraformaldehyde fixed cells, exposed to media or 400 nM cRGDY-PEG-Cy5-C' dots, and treated with methylene blue reagent (1 mL; 1 hr, 37 °C), as a measure of cellular attachment. Table of (C, right) shows associated p values. For each ligand number, triplicate assays were performed for each concentration and time point.

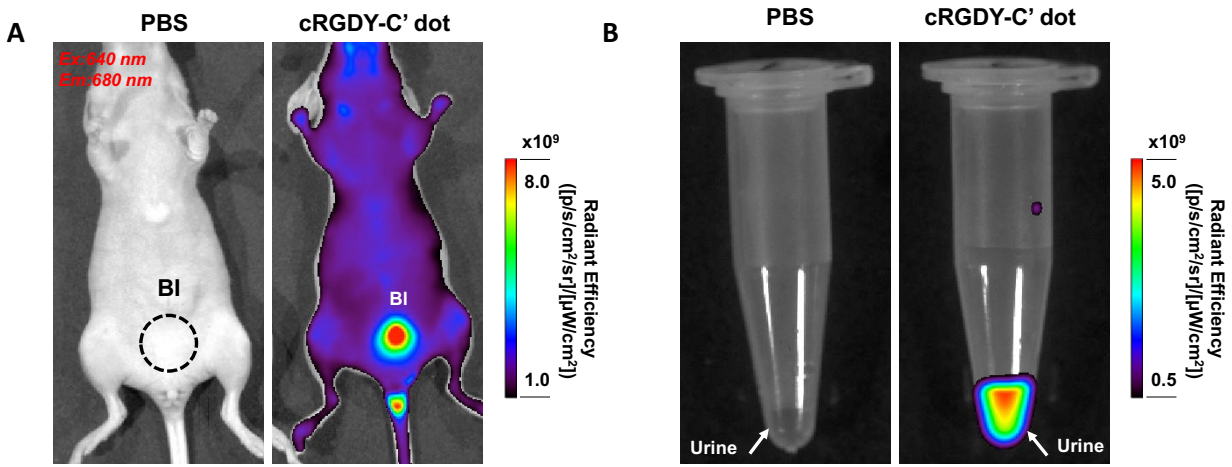

Figure S9. Optical imaging of renal clearable cRGDY-PEG-Cy5-C' dots (18 cRGDY/C' dot). (A) IVIS spectrum whole-body optical images of mice injected intravenously with either phosphate buffered saline (PBS, left) or cRGDY-PEG-Cy5-C' dots (1.5 nmol, right) at 20 min post-injection. BI: bladder. (B) Optical images of urine specimens taken from corresponding mice. For all optical imaging studies, the excitation and emission filters were set to be 640 nm and 680 nm, respectively.

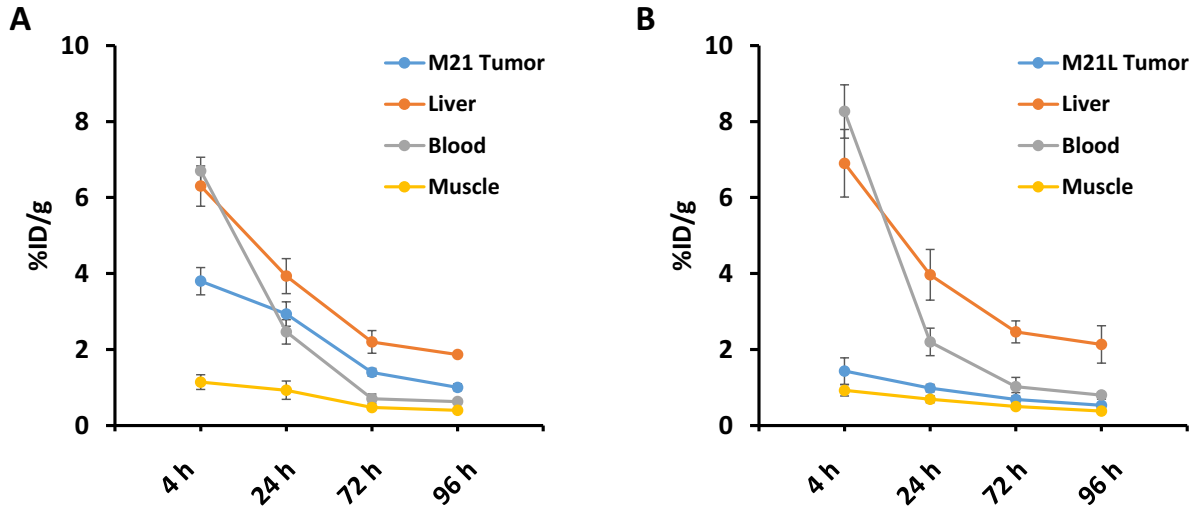

Figure S10. Time activity curves of blood and tissue specimens harvested from (A) M21 tumor-bearing mice, and (B) M21L tumor-bearing mice injected with ^{124}I-cRGDY-PEG-Cy5-C' dots (18 cRGDY/C' dot).

Table S1. Results of quantitative analysis of GPC elugrams of cRGDY-PEG-Cy5-C' dots.

			Before purification				After purification			
			Mean Elution time (min)	Peak area / purity	Diameter by FCS	Single-particle brightness by FCS	Mean Elution time (min)	Peak area / purity	Diameter by FCS	Single-particle brightness by FCS
Representative Synthesis (Fig. 1B and C)	Fraction 1 (green)	Peak 1	5.8	11.1 %	19.3 nm	5 kHz				
		Peak 2	6.1	5.4 %						
	Fraction 2 (red)	Peak 3	8.9	72.6 %	6.4 nm	13 kHz	8.9	100 %	6.4 nm	13 kHz
	Fraction 3 (blue)	Peak 4	12.5	10.9 %	2.3 nm	5 kHz				
Example of failed synthesis in which particles aggregate (Fig. 1E and F)	Fraction 1 (green)	Peak 1	5.9	11.1 %	21.2 nm	5 kHz				
	Fraction 2 (red)	Peak 2	8.1	66.8 %	7.8 nm	16 kHz	7.8	46 %	7.7 nm	11 kHz
		Peak 3	8.8	22.1 %			8.7	54 %		
	Fraction 3 (blue)	Peak 4	NA	<0.1%	NA	NA				

Table S2. Pharmacokinetic-derived activities and half-lives of ^{131}I-cRGDY-PEG-Cy5-C' dots with varying ligand numbers in a human melanoma (M21) xenograft model

	6 cRGDY/C' dot						14 cRGDY/C' dot						18 cRGDY/C' dot					
	Activity (%ID/g)		Biological Half-life		Effective Half-life		Activity (%ID/g)		Biological Half-life		Effective Half-life		Activity (%ID/g)		Biological Half-life		Effective Half-life	
Target Organ	$A_{0,1}$	$A_{0,2}$	$(T_{1/2})_1$	$(T_{1/2})_2$	$(T_{1/2})_1$	$(T_{1/2})_2$	$A_{0,1}$	$A_{0,2}$	$(T_{1/2})_1$	$(T_{1/2})_2$	$(T_{1/2})_1$	$(T_{1/2})_2$	$A_{0,1}$	$A_{0,2}$	$(T_{1/2})_1$	$(T_{1/2})_2$	$(T_{1/2})_1$	$(T_{1/2})_2$
Blood	17	6	3.5	22	3.38	17.9	20	7	2.6	16	2.53	13.7	18.5	1	3.5	22	3.38	17.9
Tumor	4.3	-	1.8	44	1.77	30.2	4.8	-	1.8	27	1.77	21.1	3	1.6	1.5	48	1.48	32.1
Heart	4	2.2	1.5	35	1.48	25.7	4.1	1.9	3	32	2.91	24	4	0.82	2.6	36	2.53	26.2
Lungs	5.7	3.3	3.1	42	3	29.3	6.5	3.3	3.7	31	3.56	23.5	6	1.05	4.5	42	4.3	29.3
Liver	1.4	3	4	116	3.84	52.7	0.6	4.3	4	73	3.84	41.6	3.3	3.2	6	190	5.65	64
Spleen	1.1	2.2	1.9	148	1.86	58.4	5.7	-	1.6	78	1.57	43.1	1.5	4.7	3	240	2.91	68.8
Stomach	10	1.15	1.33	42	1.31	29.3	1.4	2.8	4	19	3.84	15.9	9	0.55	1.4	42	1.38	29.3
S. Int.	1.75	1.3	1	39	0.99	27.8	2.3	-	28	-	21.7	-	1.95	0.85	3	48	2.91	32.1
L. Int.	0.55	1.55	6	52	5.65	33.8	0.35	2	6	35	5.65	25.7	1.3	0.95	4	42	3.84	29.3
Kidneys	0.8	1.6	1.9	50	1.86	32.9	2.2	3	7	48	6.53	32.1	4	2.1	6	92	5.65	47.1
Muscle	1.15	-	42	-	29.3	-	1.15	-	32	-	24	-	0.9	0.3	6	52	5.65	33.8
Bone	1.8	1.1	1.7	60	1.67	37	1.35	1.5	3	34.6	2.91	34.6	1.8	0.73	3	120	2.91	53.5

"Activity, A_0," for the targeted probe (^{131}I-cRGDY-PEG-C' dots) refers to the zero-time intercept of the fitted time-activity concentration curve. Units of activity are indicated as the percentage of the ID per gram (%ID/G) of tissue.

Table S3. Integrated activity of ^{131}I-cRGDY-PEG-Cy5-C' dots in a 70-kg standard man

	Integrated Activity (μCi-h/μCi)		
Tissue	**6 cRGDY/C' dot**	**14 cRGDY/C' dot**	**18 cRGDY/C' dot**
Lower Large Intestine contents	0.11	0.10	0.06
Small Intestine contents	0.14	0.07	0.11
Stomach contents	0.26	0.28	0.16
Upper Large Intestine contents	0.11	0.10	0.06
Heart contents	0.10	0.09	0.05
Kidneys	0.11	0.23	0.25
Liver	1.57	1.74	2.14
Lungs	0.57	0.51	0.28
Muscle	8.75	7.19	3.96
Bone - Cortical	1.10	1.40	1.11
Bone - Trabecular	1.10	1.40	1.11
Spleen	0.12	0.15	0.30
Urinary Bladder Wall*	1.18	1.22	1.50
Biological half-time	3.50	2.60	3.50
Total Body	42.10	34.60	18.26
Rest of Body	28.07	21.34	8.65

* Assuming a voiding interval of 3 hours.

Table S4. Radiation dosimetry of i.v.-injected ^{131}I-cRGDY-PEG-Cy5-C' dots for a range of ligand numbers

Target Organ	6 cRGDY/C' dot Absorbed Dose (rem/mCi)	14 cRGDY/C' dot Absorbed Dose (rem/mCi)	18 cRGDY/C' dot Absorbed Dose (rem/mCi)
Adrenals	0.767	0.644	0.377
Brain	0.646	0.508	0.225
Breasts	0.556	0.438	0.205
Gallbladder Wall	0.839	0.704	0.441
Lower Large Intestine Wall	0.976	0.810	0.437
Small Intestine	0.909	0.702	0.397
Stomach Wall	1.00	0.883	0.48
Upper Large Intestine Wall	0.894	0.733	0.398
Heart Wall	0.761	0.622	0.322
Kidneys	0.682	0.842	0.742
Liver	0.982	0.995	1.04
Lungs	0.712	0.608	0.344
Muscle	0.599	0.490	0.264
Ovaries	0.833	0.664	0.345
Pancreas	0.831	0.690	0.400
Red Marrow	0.740	0.666	0.393
Bone	1.21	1.13	0.681
Skin	0.48	0.382	0.183
Spleen	0.830	0.855	1.19
Testes	0.662	0.522	0.255
Thymus	0.661	0.523	0.246
Thyroid	0.667	0.525	0.239
Urinary Bladder Wall	1.89	1.78	1.79
Uterus	0.895	0.720	0.404
Total Body	0.715	0.589	0.322
Effective Dose	**0.838**	**0.724**	**0.462**

The OLINDA dosimetry program yields separate absorbed-dose estimates for the upper and lower large intestine walls.